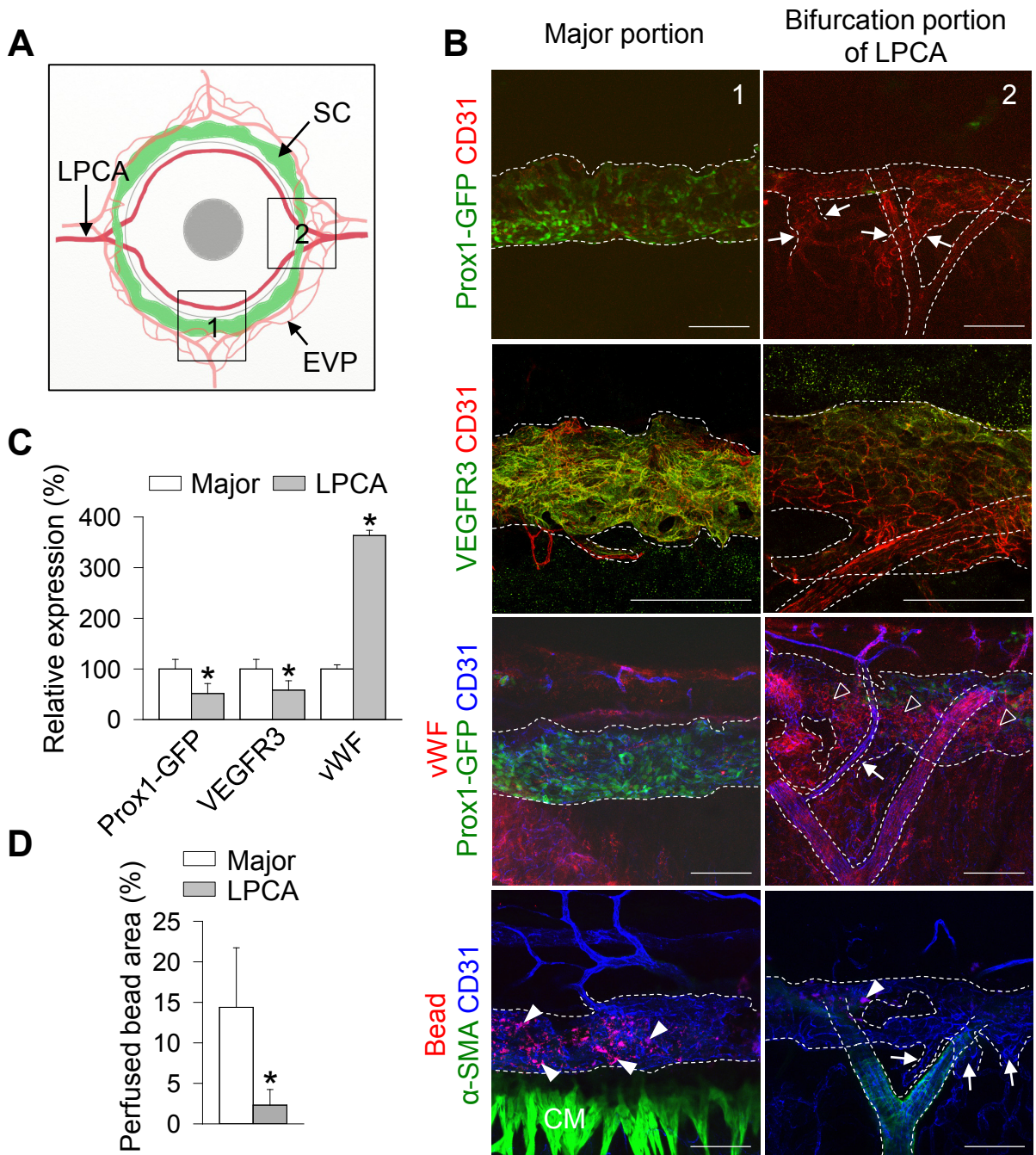


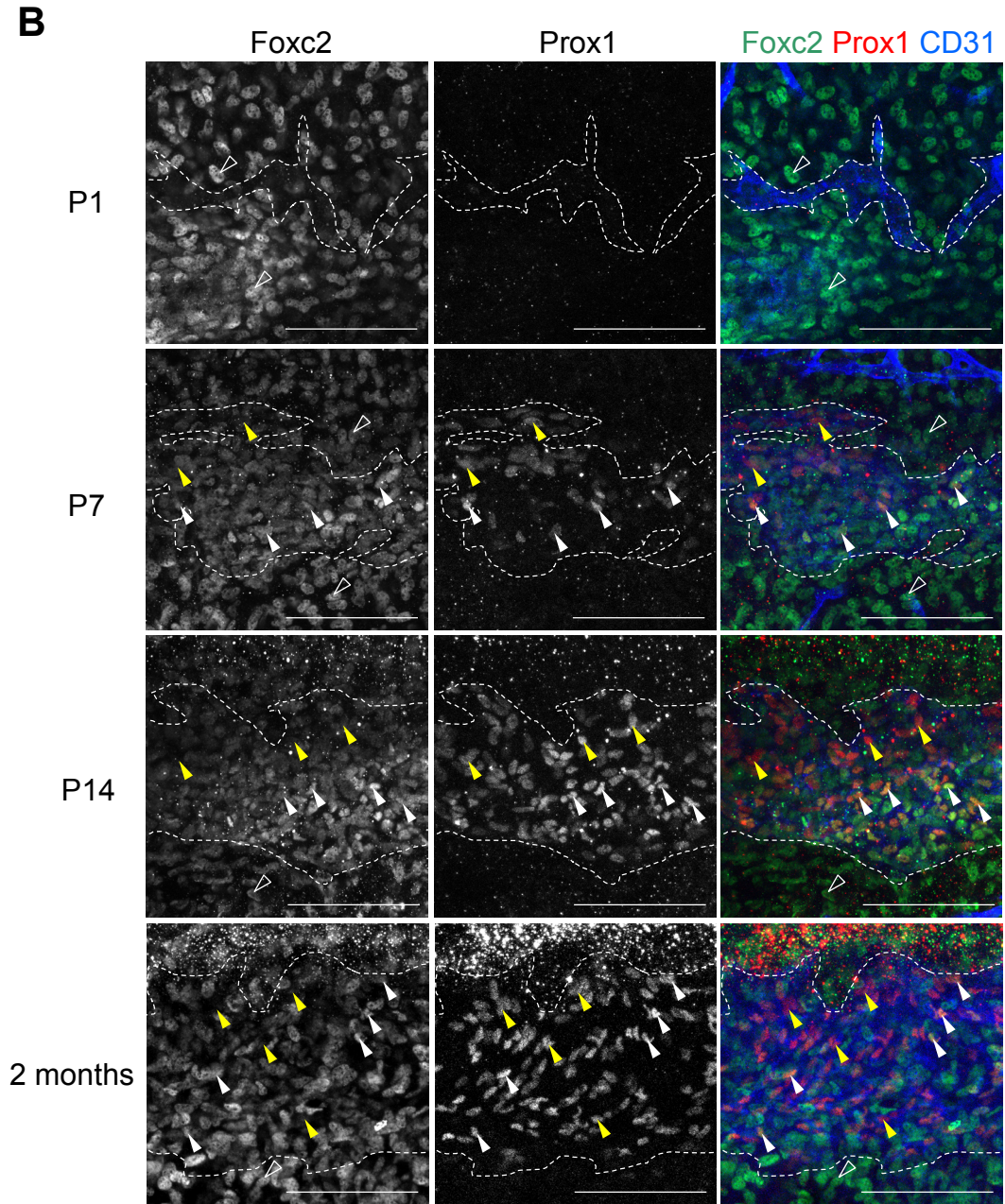
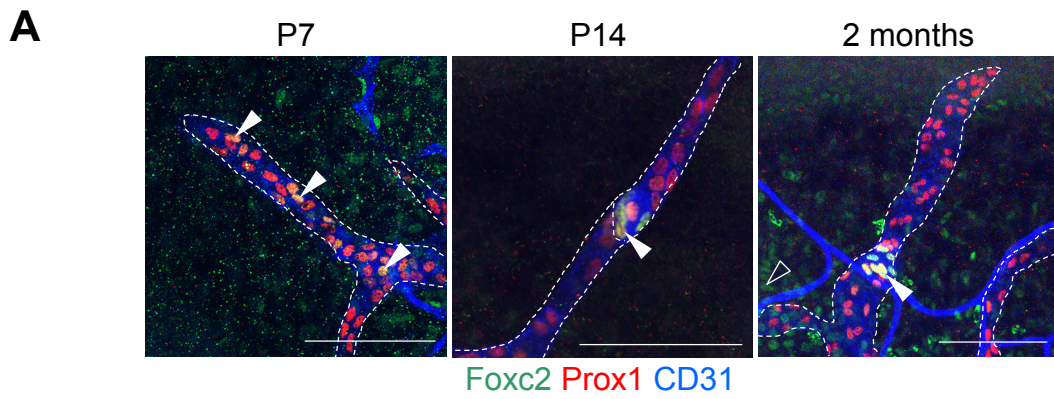
Supplemental Data

Prox1 as a biosensor reflecting the integrity of Schlemm's canal

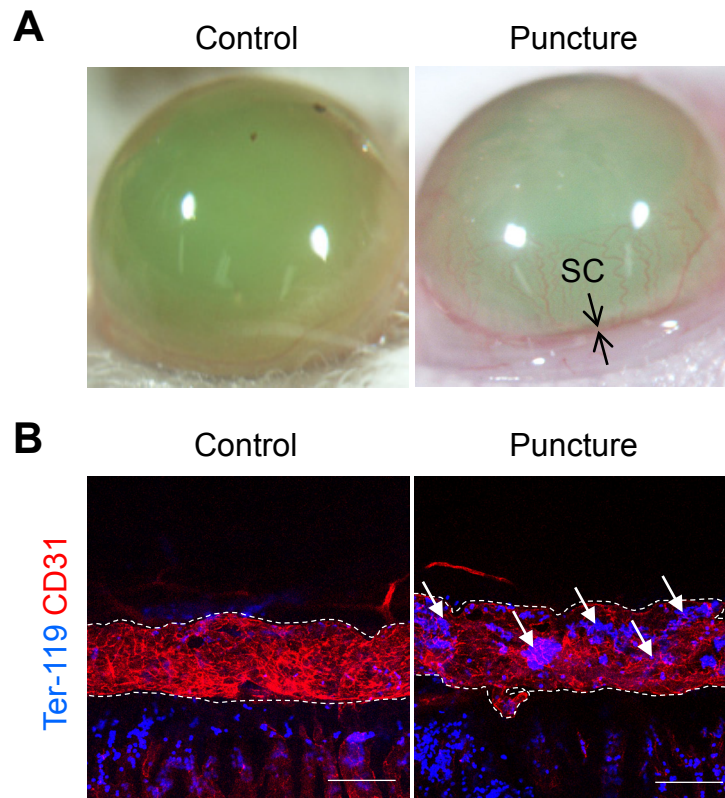
Dae-Young Park, Junyeop Lee, Intae Park, Dongwon Choi, Sunju Lee, Sukhyun Song, Yoonha Hwang, Ki Yong Hong, Yoshikazu Nakaoka, Taija Makinen, Pilhan Kim, Kari Alitalo, Young-Kwon Hong, Gou Young Koh



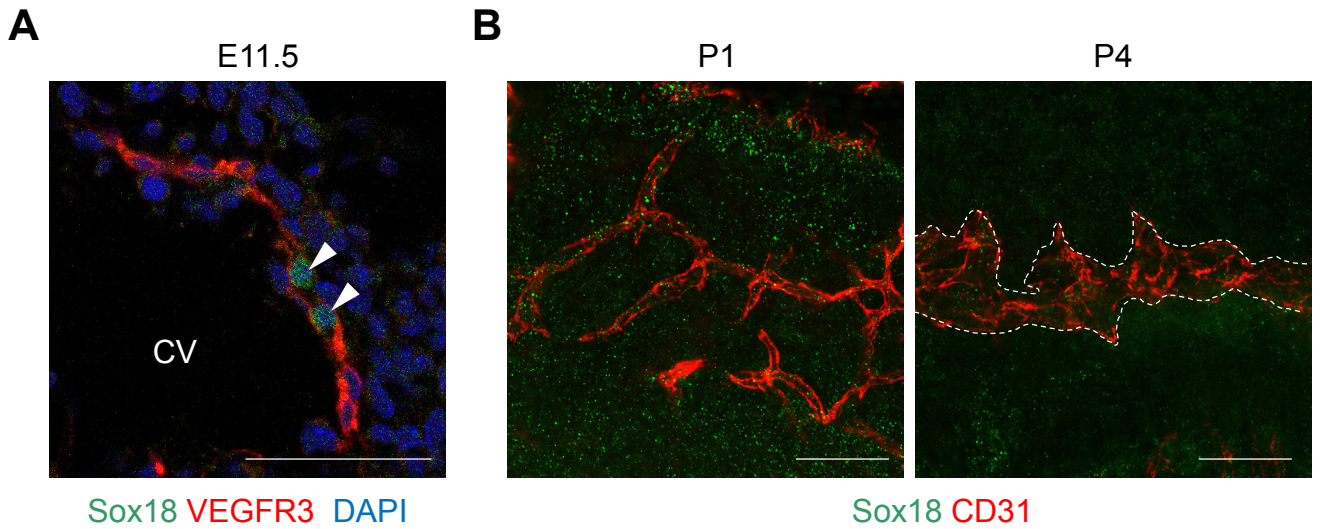
Supplemental Figure 1. SC with low Prox1 expression is normally present adjacent to the bifurcation portion of the LPCAs. (A-D) Images and comparisons of SC in the major portion and nearby the bifurcation portion of LPCAs. (A) Schematic diagram showing SC (green), LPCA (dark red) and limbal BVs (light red). Box 1 indicates a major portion of SC (Major), whereas box 2 indicates the portion of SC nearby the bifurcation of LPCAs (LPCA). EVP; episcleral venous plexus. (B) Immuno-staining for Prox1-GFP, VEGFR3, vWF, α -SMA and perfused microbead (bead) in CD31⁺ SC. Arrows indicate the remnant communication between SC and the CVs. Blank arrowheads indicate vWF expression of SC. Arrowheads indicate perfused beads in CD31⁺ SC. (C) Comparisons of relative expression in Prox1, VEGFR3 and vWF. Each group, n = 5. *p < 0.05 versus Major. The quantification of SC in the major portion was normalized to 100%, from which the quantifications of other groups were calculated. (D) Microbead⁺ perfused SC areas, presented as a percentage of CD31⁺ SC areas. Each group, n = 5. *p < 0.05 versus Major. All scale bars, 100 μ m.



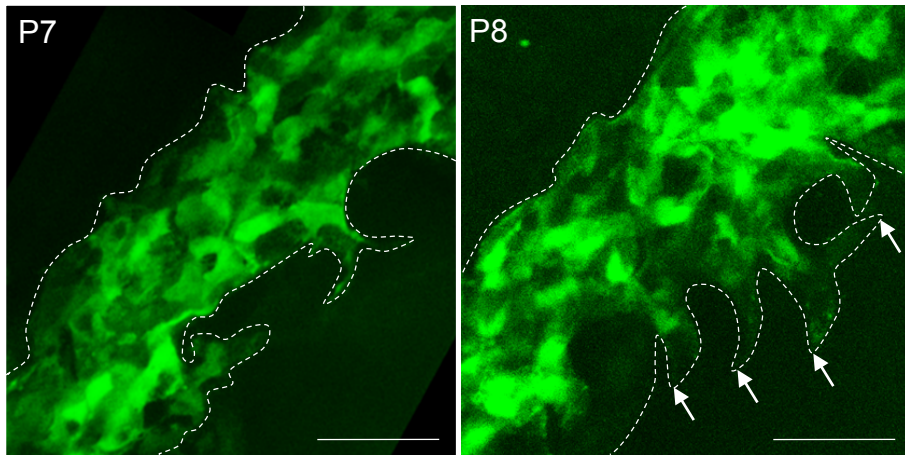
Supplemental Figure 2. Temporal changes of the expressions of Foxc2 and Prox1 in limbal LVs. (A) and SC (B) during postnatal development. White arrowheads indicate overlaps between Foxc2 and Prox1 while yellow arrowheads mark Prox1 expression without Foxc2. Blank arrowheads denote Foxc2 expression in mesenchymal cells. All scale bars, 100 μ m.



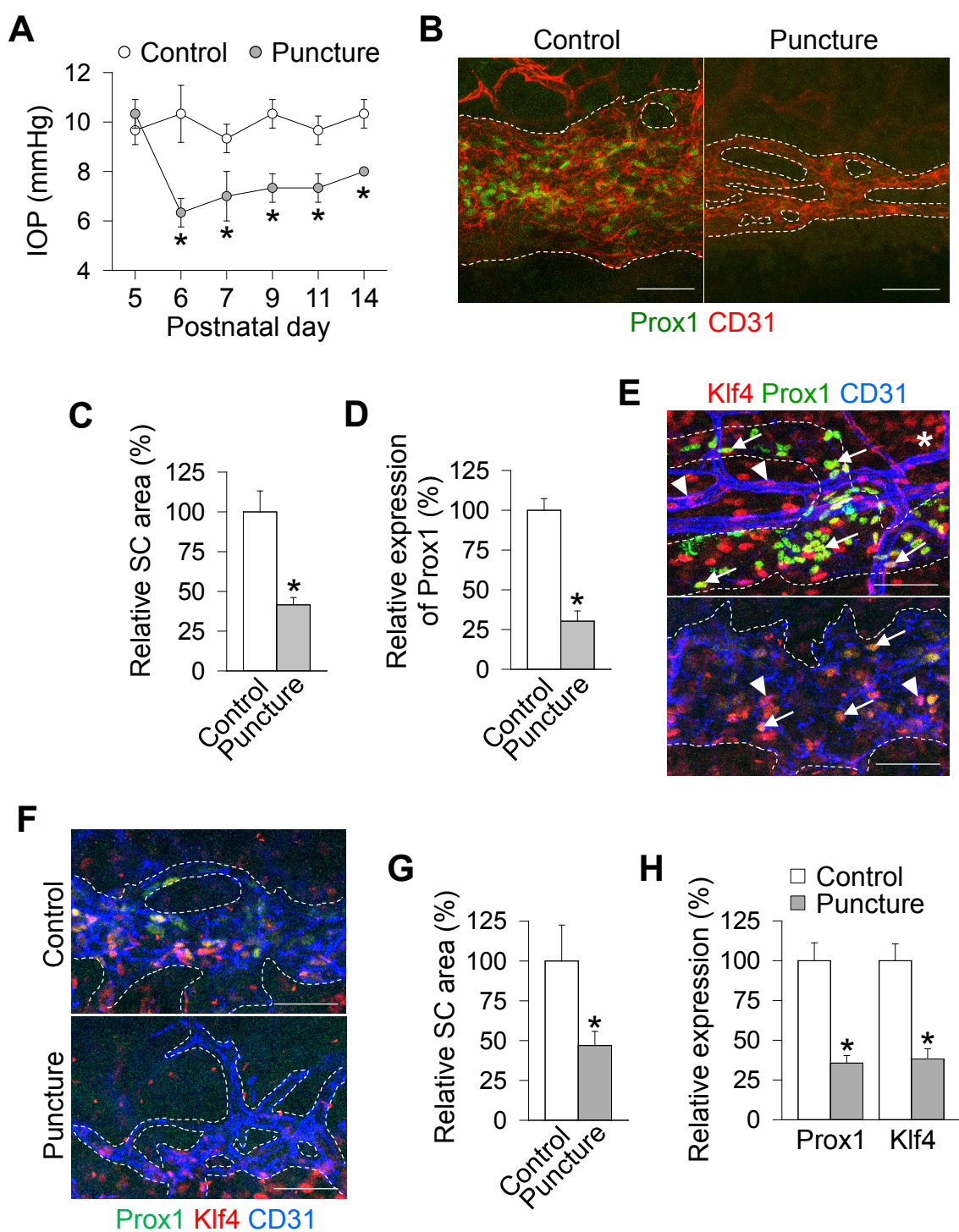
Supplemental Figure 3. SC does not include valves to prevent blood regurgitation. (A and B) Eyes of Prox1-GFP transgenic mice were punctured. (A) Appearance of cornea immediately after ocular puncture. Arrows indicate the reddish SC filled with blood. (B) Perfused Ter-119⁺ RBCs in CD31⁺ SC after ocular puncture. Scale bars, 100 μ m.



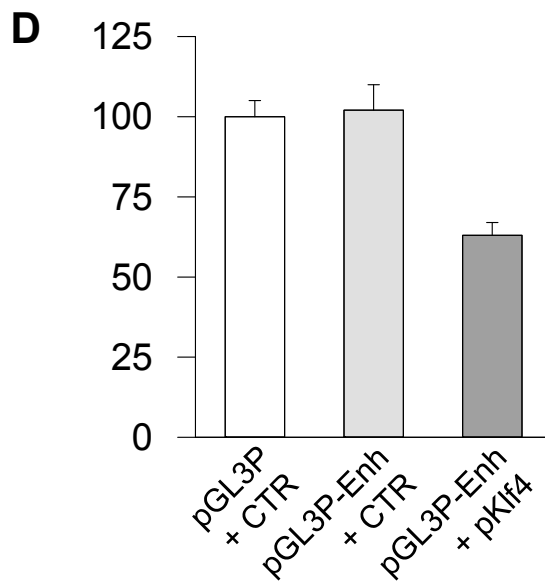
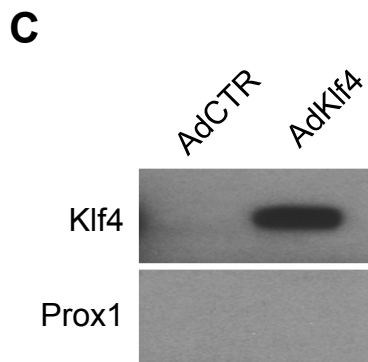
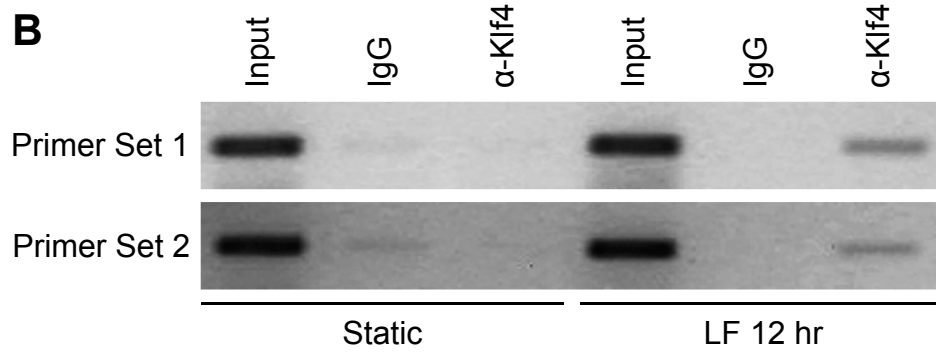
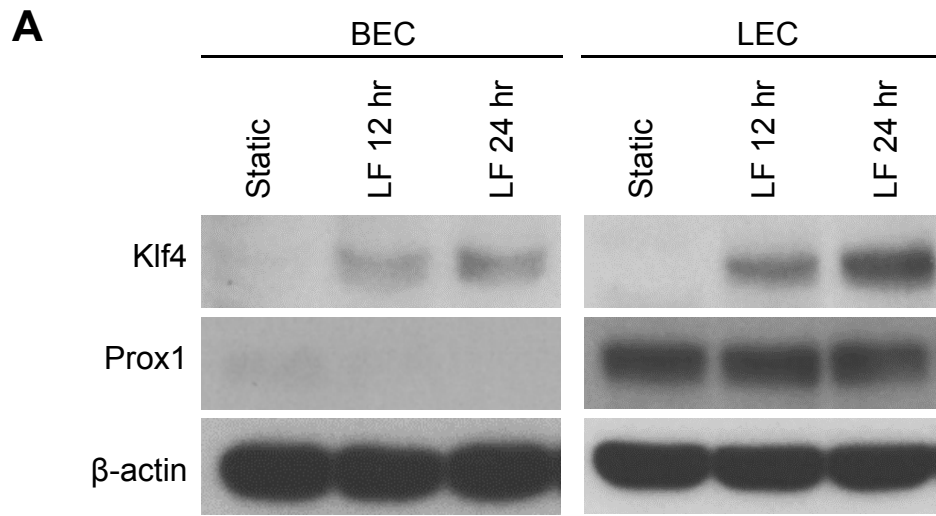
Supplemental Figure 4. Analysis of Sox18 expression in cardinal vein and SC. Images showing expression of Sox18 in VEGFR3⁺ cardinal vein (CV) at E11.5 (**A**) and CD31⁺ SC at P1 and P4 (**B**). All scale bars, 50 μ m.



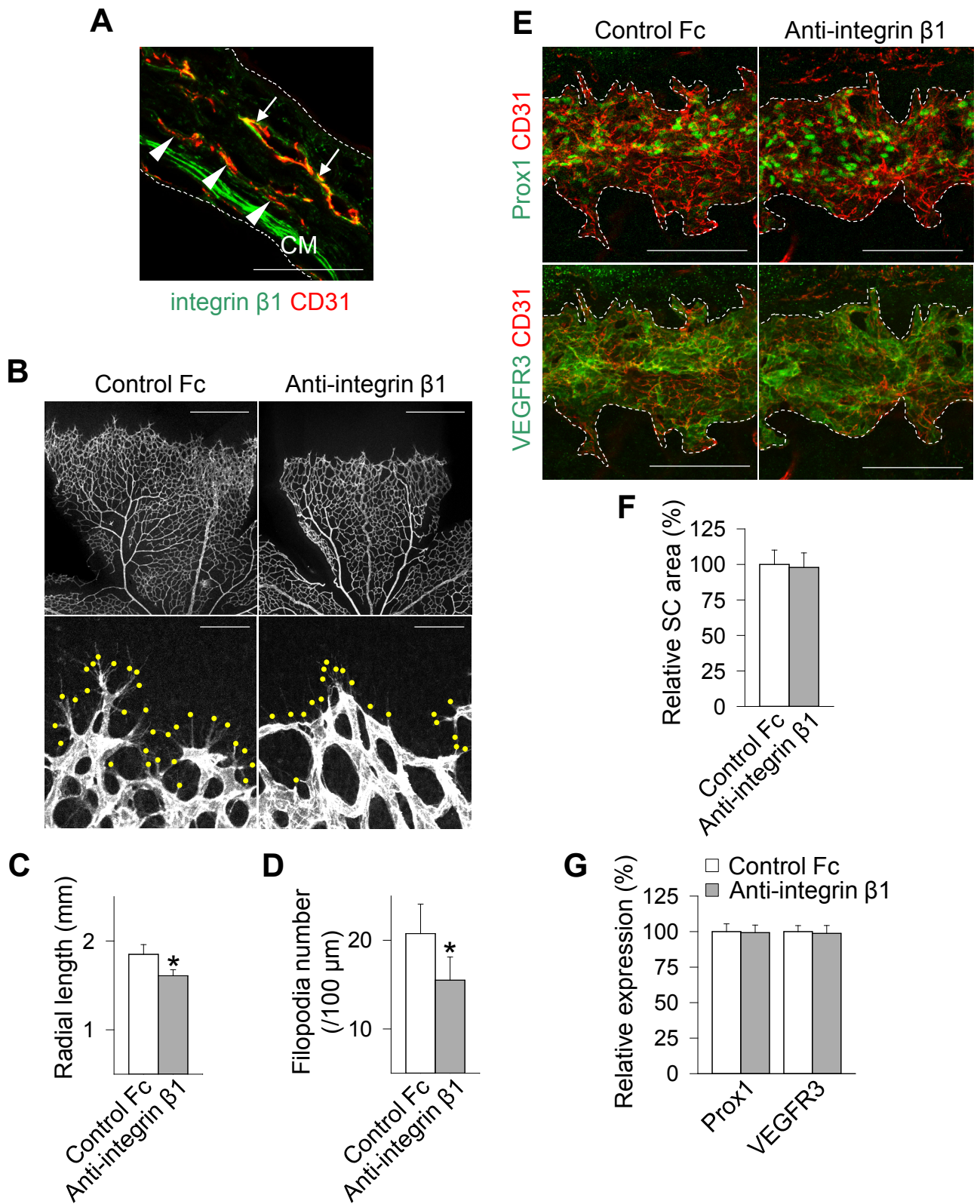
Supplemental Figure 5. Intravital imaging of SC during development. Serial images of Prox1-GFP⁺ SC at P7 and P8. Arrows indicate new sprouting from the preexisting SC. Scale bars, 50 μ m.



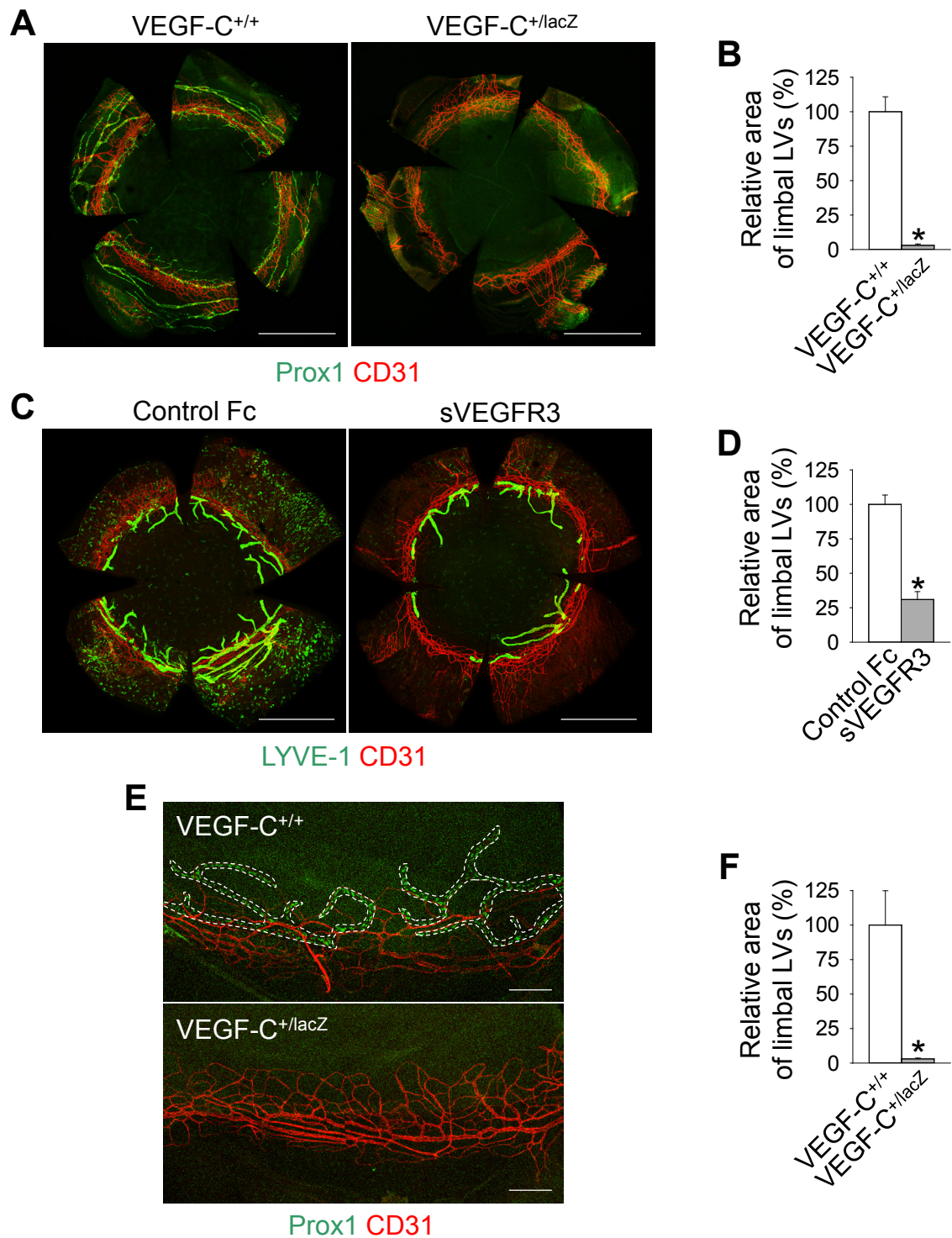
Supplemental Figure 6. Decreased AHO delays the lymphatic fate of SC during postnatal development. Unless otherwise denoted: for the bar graphs, the quantification of control group was normalized to 100%, from which the quantifications of other groups were calculated. **(A-D)** Images and comparisons of the SC between the punctured eyes versus the sham-operated non-punctured eyes. Eyes were punctured from P5 to P14 and the corneas were harvested at P14. **(A)** Comparison of IOP. Each group, $n = 4$. * $p < 0.05$ versus Control. **(B)** Images showing Prox1 expression in CD31⁺ SC. **(C and D)** Comparisons of relative area and expression of Prox1 in SC. Each group, $n = 4$. * $p < 0.05$ versus Control. **(E)** Images showing Klf4 and Prox1 in limbal LVs and BVs (upper panel), and in CD31⁺ SC (lower panel) at P5. Dashed lines demarcate limbal LVs (upper panel) and SC (lower panel), respectively. Arrows indicate co-expression of Klf4 and Prox1 in limbal LVs and SC, while arrowheads indicate sole Klf4 expression in limbal BVs and SC. Asterisks denote Klf4 expression in corneal epithelium. **(F-H)** Eyes were punctured from P3 to P4 and corneas were harvested at P5. **(F)** Images showing Prox1 and Klf4 expression in CD31⁺ SC. **(G and H)** Comparisons of relative area and expression of Prox1 and Klf4 in SC. Each group, $n = 4$. * $p < 0.05$ versus Control. All scale bars, 50 μm .



Supplemental Figure 7. Analyses of the flow-mediated Klf4 expression in BECs and LECs. (A) Western blot showing the regulation of Klf4 and Prox1 expression in human neonatal primary dermal BECs and LECs in response to laminar flow (LF) for 12 and 24 hours. Note the increased expression of Klf4, but not Prox1, in both cell types by laminar flow. β -actin was used for loading control. [Samples were run on separate gels.](#) (B) Chromatin immunoprecipitation (ChIP) was performed using an anti-Klf4 antibody (α -Klf4) against primary LECs cultured under the static or 12 hour-flow condition. IgG, normal goat IgG control. Binding of Klf4 protein to the Prox1 gene was confirmed using two independent PCR primer sets. (C) Adenoviral overexpression of Klf4 did not activate the Prox1 expression in BECs. Human neonatal primary dermal BECs was transduced with adenovirus encoding GFP (AdCTR) or Klf4 (AdKlf4) for 48 hours and subjected to western blot analyses. (D) Luciferase assay showing the absence of responsiveness of the Klf4-binding region in the Prox1 gene to Klf4 overexpression. The Prox1 intronic region, which was postulated to be bound by Klf4, was cloned in an enhancer-less luciferase reporter vector (pGL3-Promoter). This construct (pGL3-Promoter/Enhancer) was co-transfected with a Klf4-expressing vector into HEK293 cells and, after 48 hours, luciferase activity was determined. pGL3P, pGL3-Promoter; pGL3P-Enh, pGL3-Promoter/Prox1Enhancer; CTR, a control vector; pKlf4, a Klf4-expressing vector.



Supplemental Figure 8. Analysis of the role of integrin β 1 in retina and SC. (A) Image showing integrin β 1 expression in SC (arrowheads), limbal BVs (arrows) and CM. (B-G) Mice were i.p. treated with anti-integrin β 1 functional blocking antibody (Anti-integrin β 1) or isotype-matched control antibody (Control Fc) from P1 to P6 and harvested at P7. (B) Images showing CD31⁺ BVs in retina. Lower panels display high-magnification images of the angiogenic front. Dots indicate filopodia. Scale bars; upper panel: 500 μ m and lower panel: 50 μ m. (C and D) Comparisons of the radial length of the BVs and the number of filopodia in sprouting ECs. Each group, n = 3. *p < 0.05 versus Control Fc. (E) Images showing the expression of Prox1 and VEGFR3 in CD31⁺ SC. Scale bars, 100 μ m. (F and G) Comparisons of relative area and expressions of Prox1 and VEGFR3 in SC. Each group, n = 3. *p < 0.05 versus Control Fc. The quantification of Control Fc was normalized to 100%, from which the quantifications of other groups were calculated.



Supplemental Figure 9. VEGF-C/VEGFR3 system plays a crucial role in the development of limbal LVs. Unless otherwise denoted: for the bar graphs, the quantification of VEGF-C^{+/+} or Control Fc group was normalized to 100%, from which the quantifications of other groups were calculated. **(A and B)** Images and comparison of relative area in limbal LVs between VEGF-C^{+/lacZ} and VEGF-C^{+/+} mice at P7. Each group, n = 4. *p < 0.05 versus VEGF-C^{+/+}. **(A)** Immunohistochemistry of cornea stained for Prox1 and CD31. **(C and D)** Mice were i.p. given sVEGFR3 (25 mg/kg) daily from P1 to P6 and designated as Control Fc and sVEGFR3 and corneas were harvested at P7. **(C)** Immunohistochemistry of cornea stained for LYVE-1 and CD31. **(D)** Comparison of relative area in limbal LVs. Each group, n = 4. *p < 0.05 versus Control Fc. **(E and F)** Images and comparison of relative area in limbal LVs between VEGF-C^{+/lacZ} and VEGF-C^{+/+} mice at 1 month. Each group, n = 4. *p < 0.05 versus VEGF-C^{+/+}. **(E)** Images showing Prox1 and CD31 staining of corneas. Dashed lines demarcate Prox1⁺ limbal LVs. All scale bars, 200 μ m.

Supplemental Table 1. Representative genes that are regulated in human dermal primary BECs that were exposed to laminar flow (~2 dyne/cm²) for 12 hr.

Genes	Fold Change*	Genes	Fold Change*
ABCA7	5.41	ITGB4	57.43
ADAMTS1	6.39	KLF2	8.92
ALG13	-8.91	KLF4	9.14
ALS2CL	3.96	LCN6	69.78
APLNR	270.43	MUC4	18.36
AQP1	35.74	NPR1	6.25
ASS1	7.36	OBSCN	-180.05
C19orf33	6.16	PALM	3.56
CASP5	-305.79	PDE9A	11.08
CCDC108	229.32	PLCB4	71.73
CCDC69	4.95	PTGDS	85.23
CLEC3B	42.50	RAMP2	4.75
CLIC3	9.29	RNASE1	3.63
CMKLR1	599.83	RP11-69I8.3	-8.88
CXCR4	-7.23	S100A2	6.12
ELN	78.89	S100A4	5.24
FAM167B	5.40	SLC9A3R2	4.49
GGT1	6.09	SLCO2A1	6.85
H19	27.44	SNCAIP	-11.76
HSPA12B	14.31	TCF15	6.71
IGFBP5	24.42	ZFAT	-7.39
ISG20	5.23	ZNF467	8.10

*Fold change is fold differences in flow-exposed BECs over static BECs with p < 0.05.

Supplemental Movie 1. A 3D reconstruction of SC (green), AV (orange), limbal LVs (blue), and limbal BVs (red) in mouse corneal limbus.